nature neuroscience

SUPPLEMENTARY INFORMATION

https://doi.org/10.1038/s41593-019-0370-y

In the format provided by the authors and unedited.

Control of tumor-associated macrophages and T cells in glioblastoma via AHR and CD39

Maisa C. Takenaka[1,10], Galina Gabriely[1,10], Veit Rothhammer[1], Ivan D. Mascanfroni[1], Michael A. Wheeler[1], Chun-Cheih Chao[1], Cristina Gutiérrez-Vázquez[1], Jessica Kenison[1], Emily C. Tjon[1], Andreia Barroso[1], Tyler Vandeventer[1], Kalil Alves de Lima[1], Sonja Rothweiler[2], Lior Mayo[1], Soufiene Ghannam[3], Stephanie Zandee[3], Luke Healy[4], David Sherr[5], Mauricio F. Farez[6,7], Alexandre Prat[3], Jack Antel[4], David A. Reardon[8], Hailei Zhang[9], Simon C. Robson[2], Gad Getz[9], Howard L. Weiner[1] and Francisco J. Quintana[1,9]*

[1]Ann Romney Center for Neurologic Diseases, Brigham and Women's Hospital, Harvard Medical School, Boston, MA, USA. [2]Divisions of Gastroenterology, Hepatology and Transplantation, Beth Israel Deaconess Medical Center, Harvard Medical School, Boston, MA, USA. [3]Neuroimmunology Research Lab., Center for Excellence in Neuromics, Department of Neuroscience, Université de Montréal, Montréal, Québec, Canada. [4]Neuroimmunology Unit, Montreal Neurological Institute, Department of Neurology and Neurosurgery, McGill University, Montreal, Québec, Canada. [5]Dept of Environmental Health, Boston University School of Public Health, Boston, MA, USA. [6]Center for Research on Neuroimmunological Diseases (CIEN), Raúl Carrea Institute for Neurological Research (FLENI), Buenos Aires, Argentina. [7]Center for Epidemiology, Biostatistics and Public Health (CEBES), Raúl Carrea Institute for Neurological Research (FLENI), Buenos Aires, Argentina. [8]Center for Neuro-Oncology, Dana Farber Cancer Institute, Brigham and Women's Hospital, Boston, MA, USA. [9]The Broad Institute of MIT and Harvard, Cambridge, MA, USA. [10]These authors contributed equally: Maisa C. Takenaka, Galina Gabriely.
*e-mail: fquintana@rics.bwh.harvard.edu

Supplementary Figure 1

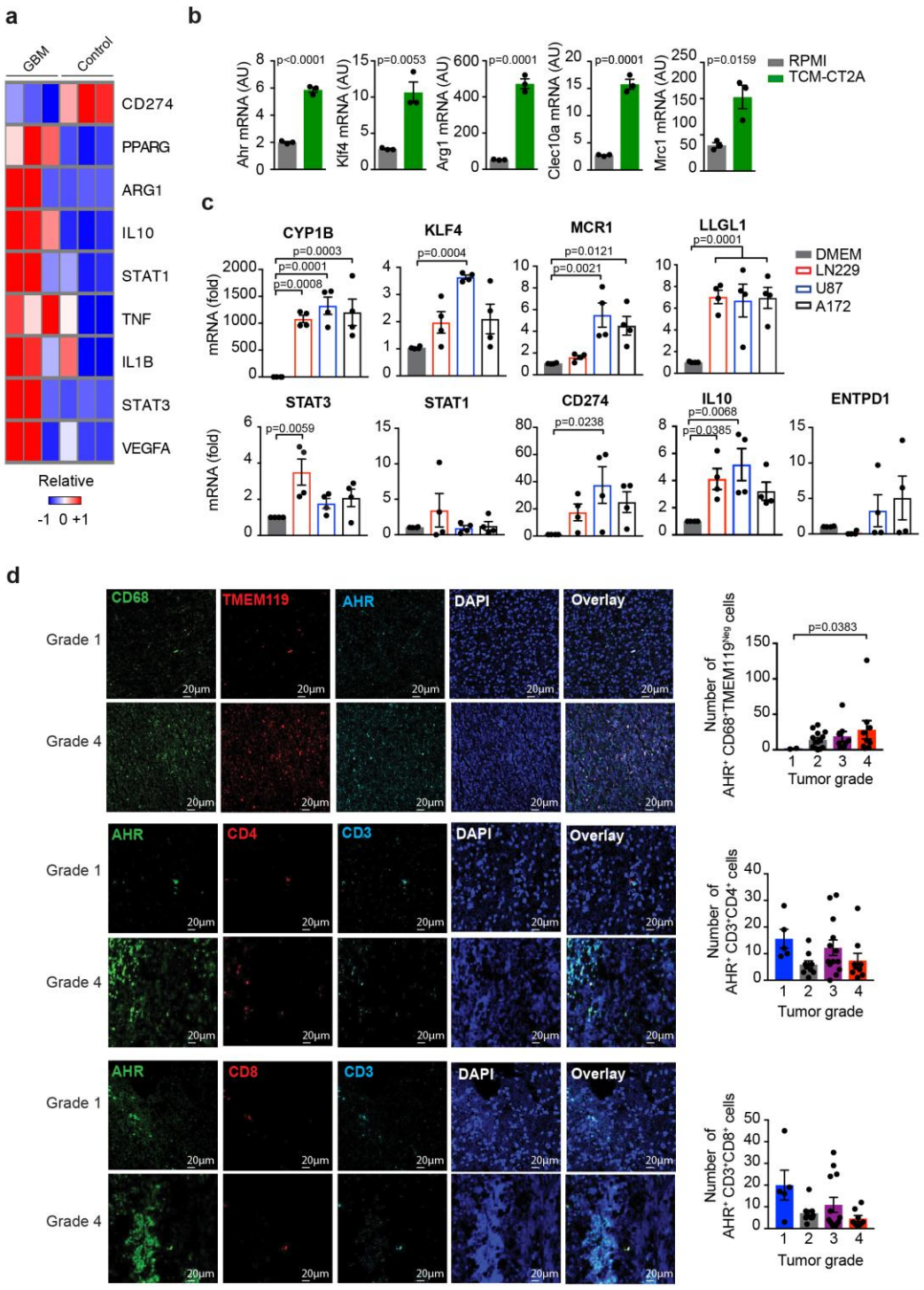

Supplementary Figure 1

Effect of TCM on human macrophages

(a) Heatmap of M1- and M2-like genes in GBM-infiltrating $CD14^+$ cells (GBM) and microglia from healthy individuals (Control) using Nanostring (n=3 biologically independent samples). **(b)** Expression of *Ahr* and M2-like genes in BMDMs stimulated with TCM from CT2A cells per 24 hours (n=3 technical replicates). Data are representative of two independent experiments with similar results. Unpaired two-tailed *t* test was used for statistical analysis. **(c)** Relative gene expression of *CYP1B*, *KLF4*, *MCR1*, *LLGL1, STAT3, STAT1, CD274, IL10* and *ENTPD1* in $CD14^+$ blood cells from healthy donors treated with TCM from different glioma cell lines per 24 hours. DMEM sample was used as reference sample. Each symbol represents an individual (n=4 biologically independent samples). Ordinary one-way ANOVA was used for statistical analysis. **(d)** Left panels. Representative immunofluorescence images of human gliomas stained for in the top CD68 (green), TMEM119 (red), AHR (cyan) and nucleus (blue), in the middle AHR (green), CD4 (red), CD3 (cyan) and nucleus (blue) and in the bottom AHR (green), CD8 (red), CD3 (cyan) and nucleus (blue). Right panels. Quantification of $AHR^+CD68^+TMEM119^{Neg}$ cells in tumor from grade 1 (n=2), grade 2 (n=14), grade 3 (n=8) and grade 4 (n=9) (top); $AHR^+CD4^+CD3^+$ cells (middle) and $AHR^+CD8^+CD3^+$ cells (bottom) in tumor from grade 1 (n=5), grade 2 (n=9), grade 3 (n=13) and grade 4 (n=8). Each symbol represents one individual and all data are mean ± s.e.m. Kruskal-Wallis test was used for statistical analysis. Scale bars, 20 μm.

Supplementary Figure 2

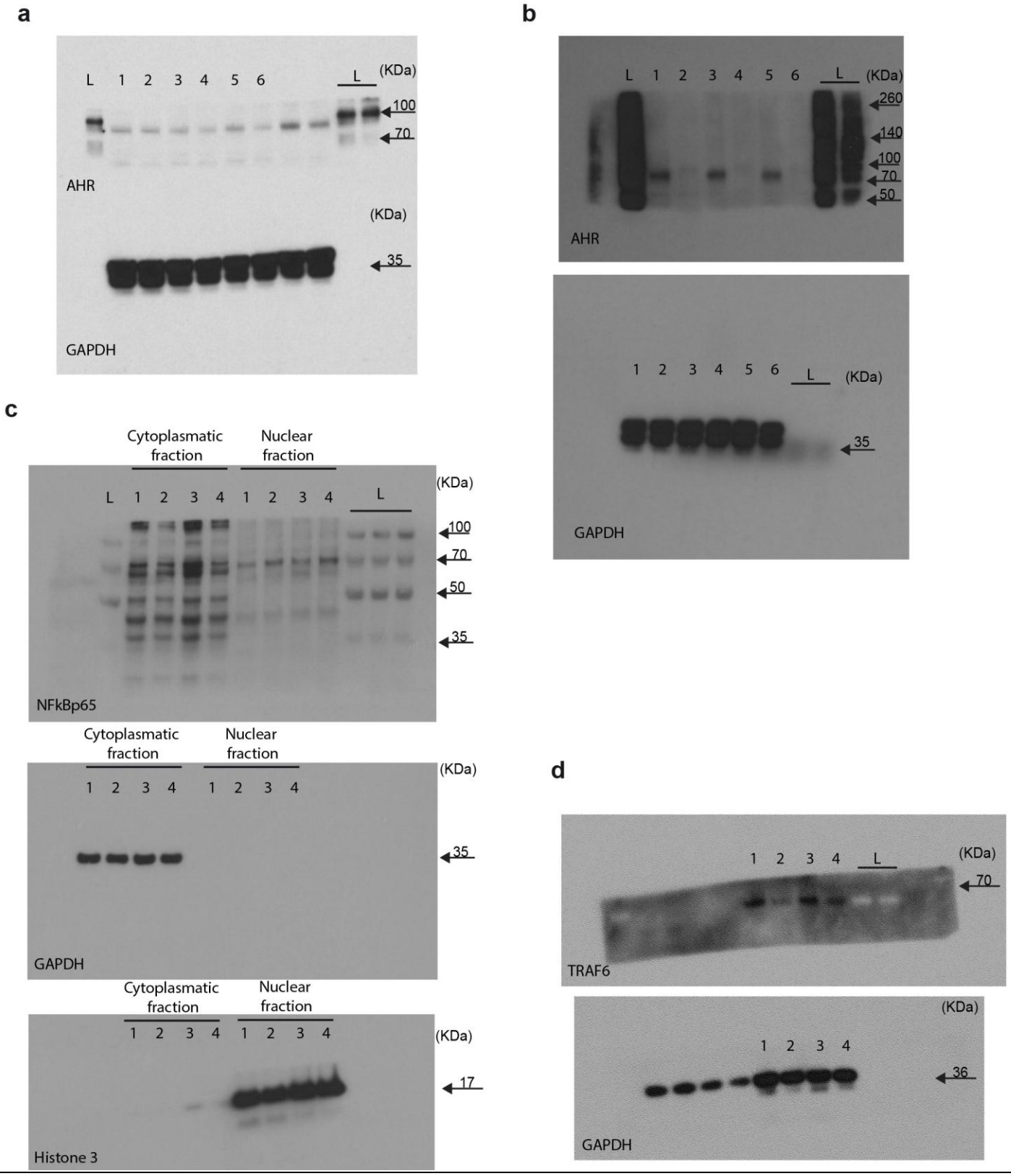

Supplementary Figure 2

Immunoblot analysis of AHR, NFkBp65 and TRAF6

(a) Immunoblots of AHR (top) and GAPDH (bottom) in total protein lysates of RAW264.7 macrophages overexpressing or not the miR-29b, corresponding to the immunoblot in the **Fig. 2n**. Control samples (1, 3, 5), miR-29b transfected cell samples (2, 4, 6). **(b)** Representative immunoblots of AHR (upper panel) and GAPDH (lower panel) in total protein lysates of BMDMs from WT and AHR^{LysM} mice, corresponding to the immunoblot in the **Suppl. Fig. 3b.** BMDMs WT (1, 3 and 5) and AHR^{LysM} (2, 4 and 6) samples. **(c)** Western Blot analysis of NF-κB (p65) (upper panel), GAPDH (middle panel) and histone 3 (lower panel) in cytoplasmatic and nuclear fraction of BMDMs stimulated or not with TCM for 90 minutes from WT and AHR^{LysM} mice, corresponding to the immunoblot in the **Fig. 4l**. Samples: 1 (control WT), 2 (TCM WT), 3 (control AHR^{LysM}) and 4 (TCM AHR^{LysM}). **(d)** Immunoblots of TRAF6 (upper panel) and GAPDH (lower panel) in total protein lysates of BMDMs stimulated or not with TCM for 6 hours from WT and AHR^{LysM} mice, corresponding to the immunoblot in the **Suppl. Fig. 4k.** Samples: 1 (control WT), 2 (TCM WT), 3 (control AHR^{LysM}) and 4 (TCM AHR^{LysM}). L: ladder**.**

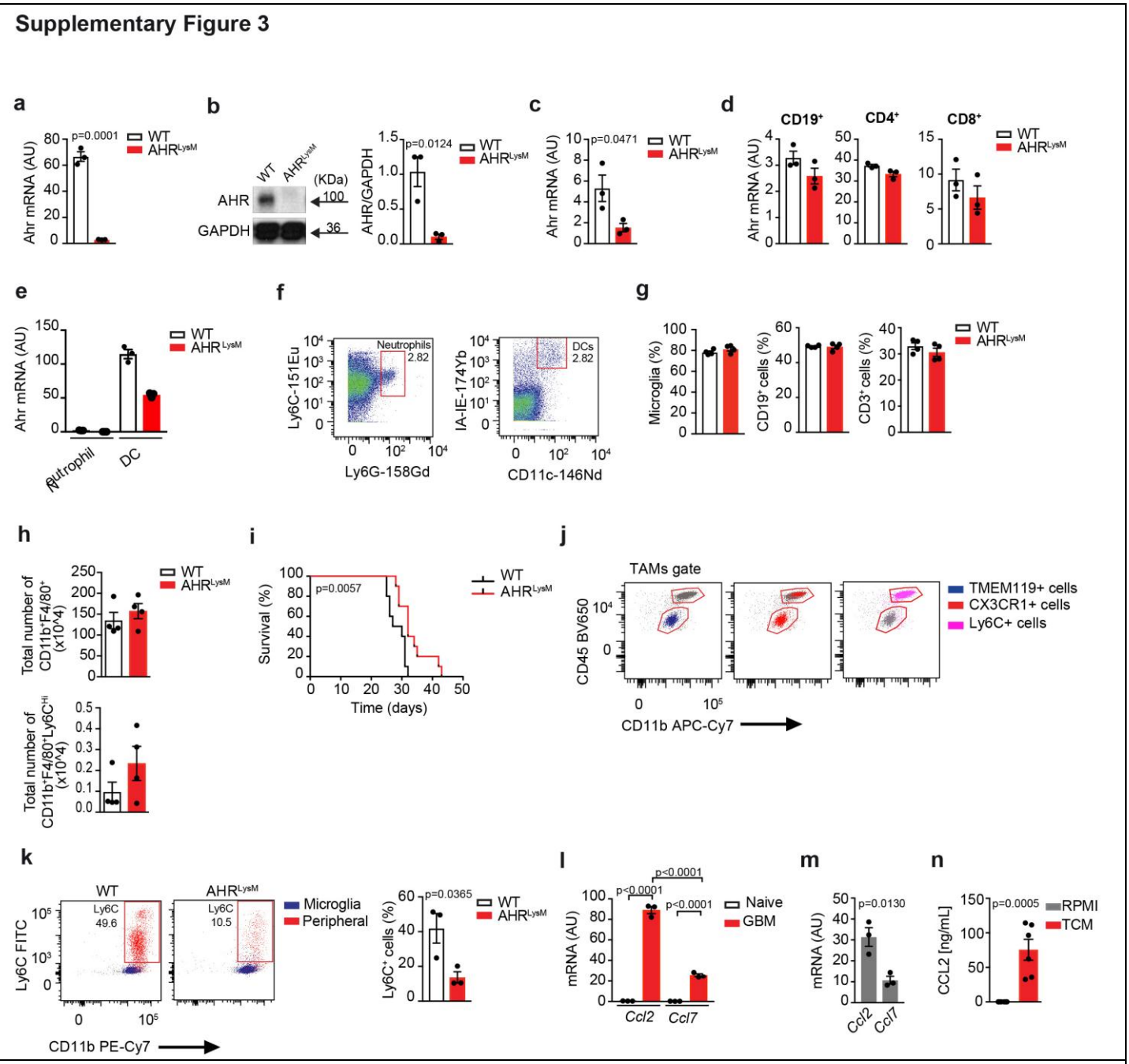

Supplementary Figure 3

AHR expression in WT and AHR^{LysM} mice

(a) *Ahr* expression in sorted bone marrow inflammatory monocytes (CD3^{Neg}B220^{Neg}Ly6G^{Neg} NK1.1^{Neg}Siglec-F^{Neg}CD11b^{+}Ly6C^{Hi}) from naive WT and AHR^{LysM} mice (n=3 independent mice). Representative of two independent experiments with similar results. **(b)** Western-blot analysis of AHR in BMDMs from WT and AHR^{LysM} mice (n=3 biologically independent samples). Data are representative of two independent experiments with similar results; images were cropped and the full scans are shown in **Supplemental Figure 2b**. **(c-e)** qPCR analysis of *Ahr* expression in microglia **(c),** B cells (CD19^{+}) and T cells (CD3^{+} CD4^{+} and CD3^{+} CD8^{+}) **(d),** neutrophils (CD115^{Neg}CD11b^{+}CD11c^{Neg}Ly6G^{+}) and dendritic cells (CD115^{Neg}CD11b^{Neg}CD11c^{+} MHCII^{Hi}) **(e)** (n=3 independent mice). **(f)** Frequency of neutrophils and dendritic cells in the CD45^{+}CD11b^{+} gate of glioma-infiltrating cells. CyTOF analysis was performed in WT mice 15 days after GL261 cell implantation. The dot plot graphs are representative of two independent experiments with similar results. **(g)** Frequency of microglia, splenic B cells and T cells in naive WT and AHR^{LysM} mice (n=4 independent mice). **(h)** Total number of

macrophages (CD11b+F4/80^{+}) and inflammatory monocytes (CD11b^{+}F4/80^{+}Ly6C^{Hi}) in spleen from WT and AHR^{LysM} (n=4 independent mice). **(i)** Survival curve analysis from WT and AHR^{LysM} mice implanted intracranially with CT2A cells (n=10 independent mice). Representative of two independent experiments with similar results. Survival analysis was performed using a Kaplan-Meier plot using a log-rank (Mantel-Cox) test. **(j)** Flow cytometry analysis of TMEM119 (blue), CX3CR1 (red) and Ly6C (magenta) expression in TAMs, 15 days after GL261 implantation in WT mice. Representative of two independent experiments with similar results. **(k)** Ly6C expression on TAMs gate (Lin^{Neg}CD11b^{+}CD45^{+}) in GBM from WT and AHR^{LysM} mice on day 15 (n=3 independent mice). In the left, representative dot plot graphs of Ly6C expression in TAMs gate, where microglia (CD45^{Low}CD11b^{+}) is shown in blue and peripheral infiltrated macrophages (CD45^{Hi}CD11b^{+}) in red. Percentage of Ly6C^{+} cells in TAMs (right panel). Representative of two independent experiments with similar results. **(l, m)** *Ccl2* and *Ccl7* gene expression in naïve brain and GL261 tumor-bearing mice **(l)** and in CT2A cells **(m)** (n=3 tmice per group). Representative of two independent experiments with similar results. **(n)** Quantification of CCL2 in TCM from human GBM cells by ELISA (n=5 biologically independent samples). Unpaired two-tailed *t* test was used to compare two groups (**a-d, g, h, k, m** and **n**) and one-way ANOVA was used to compare three or more groups (**e** and **l**). All data are presented as mean ± s.e.m.

Supplementary Figure 4

a

Ingenuity Canonical Pathways	p-value	Ratio	z-score
Macrophages, Fibroblasts and Endothelial Cells in RA	2,51E-57	0,23	NaN
Toll-like Receptor Signaling	1,26E-40	0,47	-1,57
IL-12 Signaling and Production in Macrophages	5,01E-39	0,3	NaN
IL-6 Signaling	1,00E-37	0,32	0,8
NF-κB Signaling	2,51E-37	0,25	0,6
iNOS Signaling	6,31E-34	0,59	-0,2
Production of NO and ROS in Macrophages	1,26E-28	0,2	1,3
PPAR Signaling	1,00E-24	0,3	-1,73
p38 MAPK Signaling	2,51E-24	0,25	0,17
PPARα/RXRα Activation	5,02E-22	0,18	-1,98
LPS-stimulated MAPK Signaling	1,26E-21	0,28	1,04

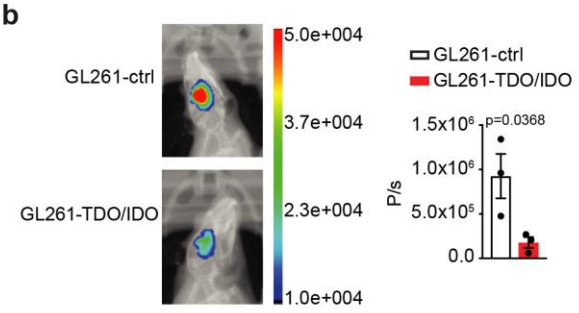

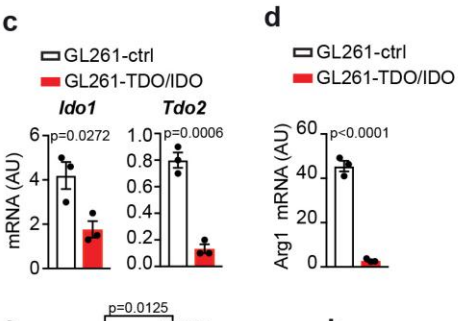

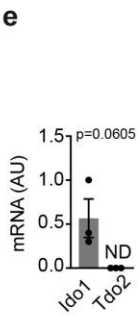

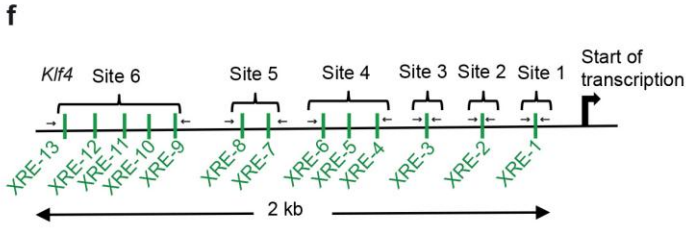

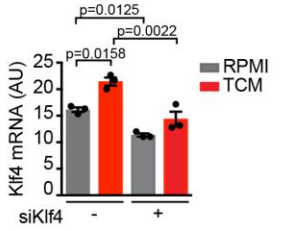

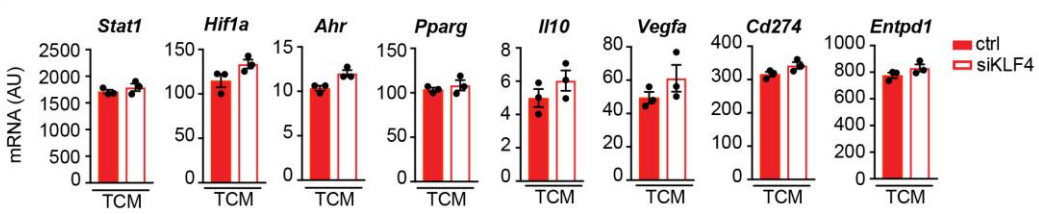

i

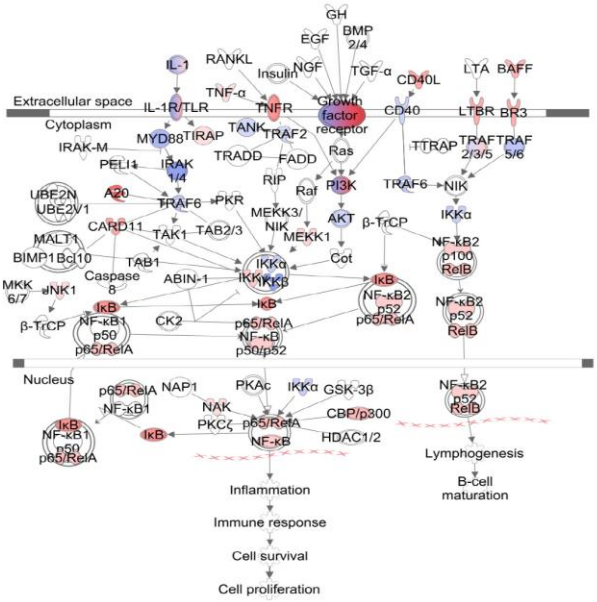

j

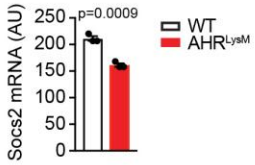

k

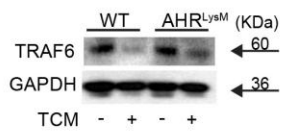

Supplementary Figure 4

Kyn regulates TAM polarization in vivo via AHR

(a) Nanostring analysis of peripheral infiltrated macrophages ($Lin^{Neg}CD11b^{+}CD45^{Hi}$) in GBM from WT and AHR^{LysM} mice 15 days after GL261 cells implantation (pool of 4 mice per group). Ingenuity pathway analysis of macrophage polarization genes is shown. **(b)** Tumor size in WT mice 7 days after implantation of GL261-control and GL261-TDO/IDO cells (n=3 independent mice). Representative images and quantification (left and right, respectively). Data are representative of two independent experiments with similar results. **(c,e)** *Ido1* and *Tdo2* expression in tumor tissue from WT mice injected with GL261- control and GL261-TDO/IDO (n=3 independent mice) **(c)**, and in CT2A cells (n=3 biologically independent samples) **(e)**. Representative of two independent experiments with similar results. **(d)** *Arg1* expression in sorted TAMs from WT mice injected with GL261-control and GL261-TDO/IDO cells (n=3 independent mice). Representative of two independent experiments with similar results. **(f)** Schematic of AHR binding sites (XREs) in the *Klf4* promoter. The arrows indicate primers designed to study AHR (sites 1-6) recruitment. **(g,h)** Klf4 gene was silenced by siRNA in bone marrow derived macrophages. The cells were stimulated with TCM from GL261 cells for 24 hours and gene expression of M1- and M2-like genes was analyzed by qPCR (n=3 technical replicates). Data are representative of two independent experiments with similar results. **(i)** Ingenuity Pathway Analysis of NF-κB signaling using data from Nanostring analysis of peripheral infiltrated macrophages ($Lin^{Neg}CD11b^{+}CD45^{Hi}$) in GBM from WT and AHR^{LysM} mice 15 days after GL261 cells implantation (pool of 4 mice per group). Colors indicate up- and down-regulation of individual pathway components in red and green, respectively. **(j,k)** *Socs2* expression **(j)** and TRAF6 protein levels **(k)** in TCM-stimulated BMDMs from WT and AHR^{LysM} mice. Data in **j** were repeated two times with similar results, with three technical replicates. The experiment in **k** was repeated two times with similar results; images were cropped and the full scans are shown in **Supplemental Figure 2d**. All data are presented as mean ± s.e.m, Unpaired two-tailed *t* test was used to compare two groups (**b-e, h** and **j**) and one-way ANOVA was used to compare three or more groups (**g**).

Supplementary Figure 5

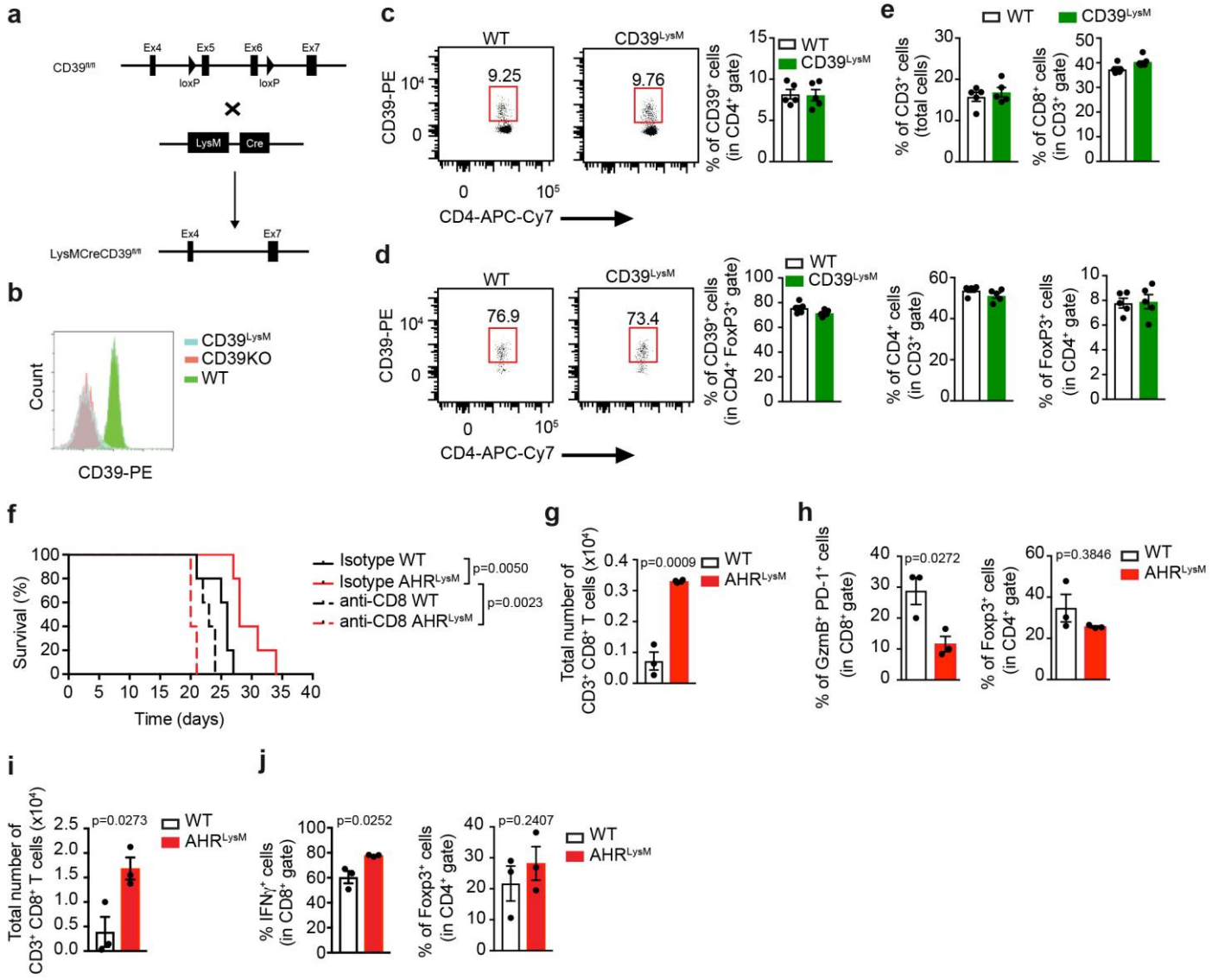

Supplementary Figure 5

CD39 in TAMs drives T cell dysfunction

(a) Schematic of generation of $LysM^{Cre}$ $CD39^{fl/fl}$ mice. There is insertion of a LoxP site into the exon 5 and the exon 6 in the mouse *Entpd1* gene. **(b)** MFI of CD39 expression determined by flow cytometry in splenic macrophages ($F4/80^+CD11b^+$) from naive WT and $CD39^{LysM}$ mice. Data are representative of two independent experiments. **(c, d)** Percentage of CD39 in $CD4^+$ T cells **(c)** and in Treg cells ($CD4^+$ $FoxP3^+$) **(d)** in the blood of WT and $CD39^{LysM}$ mice (n=5 independent mice). On the left of each figure are the representative dot plots from each group. **(e)** Frequency of $CD3^+$ T cells, $CD3^+CD8^+$ T cells, $CD3^+CD8^+$ T cells and Tregs ($FoxP3^+$ $CD4^+$) in the blood from WT and $CD39^{LysM}$ mice (n=5 independent mice). **(f)** Effect of $CD8^+$ T-cell depletion in WT and AHR^{LysM} mice performed as previously described [52]. Survival curve analysis of GBM mice injected with GL261 cells in WT and AHR^{LysM} (n=8 independent mice). Log-rank test was used to compare survival among the Isotype WT and Isotype AHR^{LysM} groups, or between Isotype and anti-CD8 treated mice in WT group or in AHR^{LysM} group. Representative of two independent experiments with similar results. **(g,h)** Flow cytometry analysis of TILs in WT and AHR^{LysM} mice 15 days after GL261 cells implantation. Total number of $CD8^+$ TILs **(g)** and frequency of PD-1^+granzyme B^+ cells in $CD8^+$ T cells and of Treg cells ($FoxP3^+$ $CD4^+$) **(h)**. Data are representative of two independent experiments with similar results, using three mice per group. **(i,j)** Flow cytometry analysis of TILs in WT and AHR^{LysM} mice 28 days after CT2A-luciferase cells implantation. Total number of $CD8^+$ TILs **(i)** and frequency of IFN-γ^+ in $CD8^+$ T cells and of Treg cells ($FoxP3^+$

$CD4^+$) **(j)**. Data are representative of two independent experiments with similar results, using three mice per group. Unpaired two-tailed *t* test was used to compare two groups (**c-e, g-j**). All data are shown as mean ± s.e.m..

Supplementary Figure 6

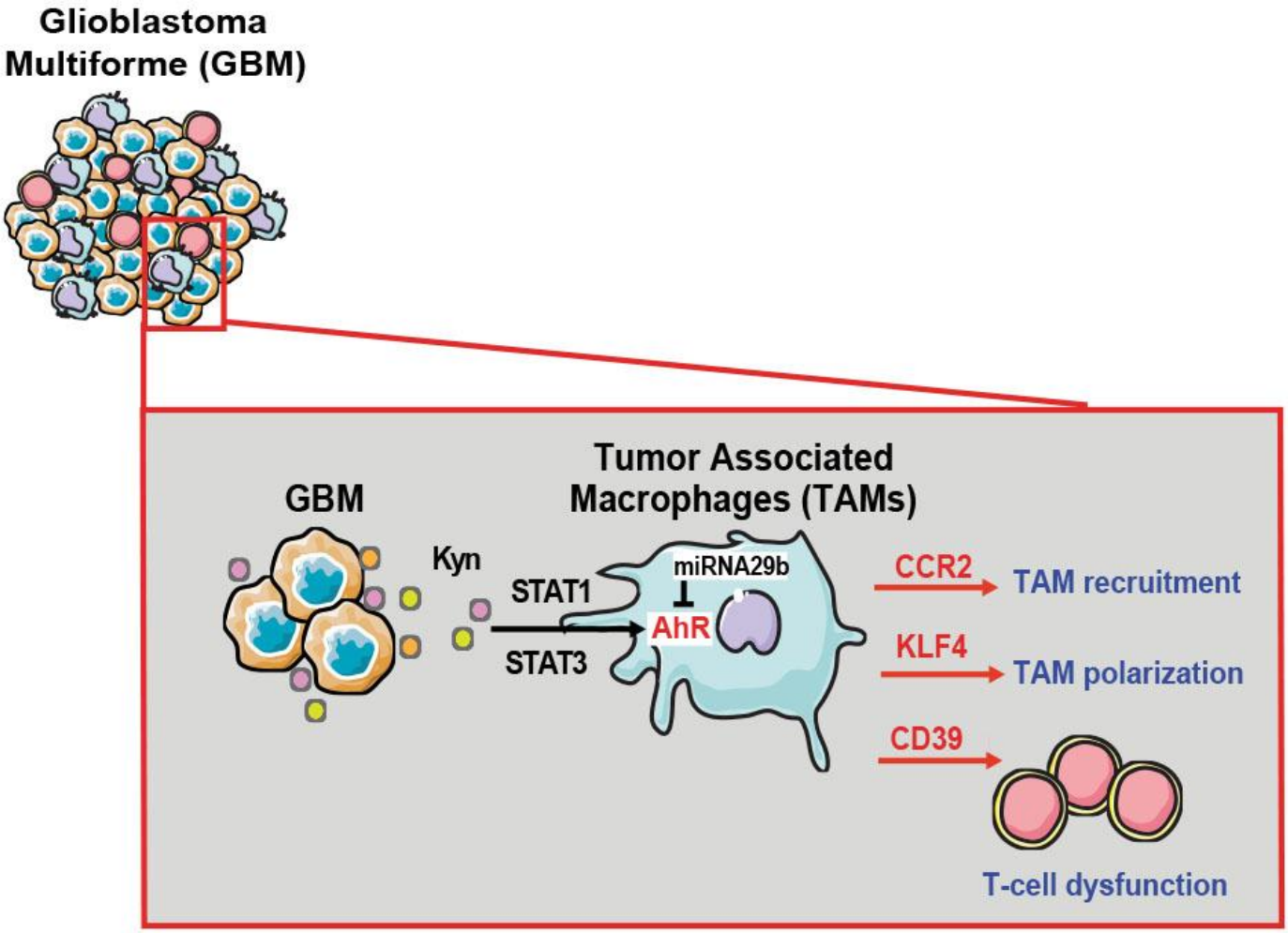

Supplementary Figure 6

Proposed model of the effects of GBM-produced AHR agonists on TAM function and T cell immunity

Kyn released by glioma cells activates AHR in TAMs, modulating TAM recruitment into GBM via CCR2, TAM polarization via KLF4/NF-κB, and T-cells via CD39.

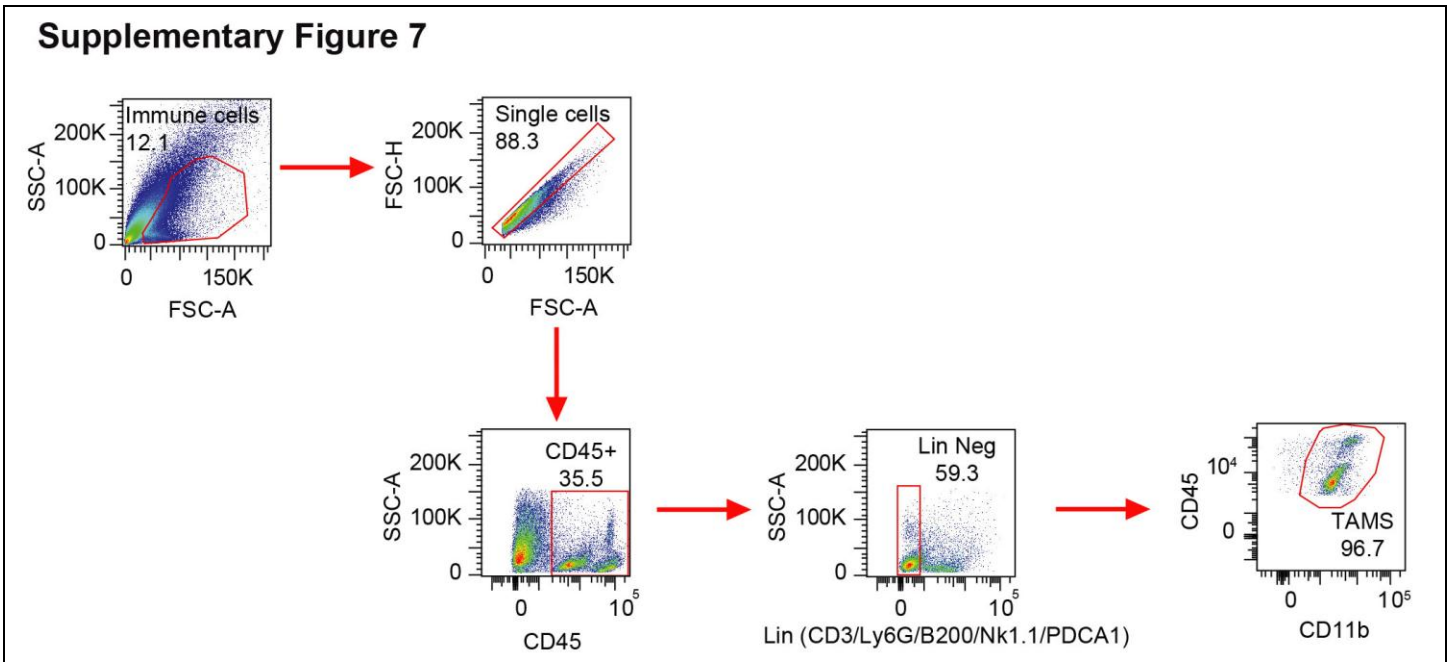

Supplementary Figure 7

Gate strategy used to analyze TAMs

FACS gating strategy for TAM purification from GBM- infiltrated mononuclear cell suspensions.

Supplementary Table 1

	Hazard Ratio	95% CI	P value
Univariate analysis			
Age	1.03	1.02 - 1.04	<0.0001
Gender (being male)	0.84	0.63 - 1.13	0.26
Karnofsky performance score (KPS)	0.97	0.96 - 0.99	<0.0001
TCGA Expression subtype			
Mesenchymal	Reference		
Proneural Non-G-CIMP	1.5	1.00 - 2.28	0.05
Proneural G-CIMP	0.28	0.14 - 0.50	<0.0001
Neural	0.77	0.49 -1.22	0.27
Classical	0.94	0.64 - 1.36	0.72
IDH1 mutated	0.35	0.17 - 0.74	0.006
MGMT methylated	0.57	0.33 - 1.00	0.05
Treatment with temozolomide (being treated)	0.54	0.41 - 0.72	<0.0001
RNA expression (high vs. low by median)			
AHR	**1.41**	**1.05 - 1.88**	**0.02**
ENTPD1	1.11	0.83 - 1.48	0.47
KLF4	1.19	0.90 - 1.58	0.23
CYP1A1	1.11	0.83 - 1.47	0.49
STAT1	1.13	0.85 - 1.50	0.39
STAT3	1.34	1.00 - 1.78	0.05
CCL2	1.45	1.09 - 1.93	0.01
CCR2	1.29	0.97 - 1.71	0.08
Multivariate model (adjusted by age, expression subtype, IDH1 mutation, KPS, and treatment)			
High *AHR* Expression	**1.7**	**1.10 - 2.63**	**0.02**
High *ENTPD1* Expression	1.58	1.02 - 2.43	0.04
High *KLF4* Expression	1.26	0.81 - 1.94	0.29
High *CYP1A1* Expression	1.2	0.78 - 1.85	0.4
High *STAT1* Expression	1.22	0.79 - 1.86	0.37
High *STAT3* Expression	1.09	0.70 - 1.69	0.7
High *CCR2* Expression	1.39	0.90 - 2.14	0.13
High *CCL2* Expression	1.44	0.94 - 2.19	0.09

Validation of univariate and multivariate analysis of overall survival using data shown in **Supplmentary Table 5** obtained from The Cancer Genome Atlas Research Network, Nature 2018, 455:2061-1068. Log-rank test was used to assign significance.